Published in final edited form as:

Proc SPIE Int Soc Opt Eng. 2016 ; 9930: . doi:10.1117/12.2236695.

Label-free molecular imaging of bacterial communities of the opportunistic pathogen *Pseudomonas aeruginosa*

Nameera Baig[a], **Sneha Polisetti**[a], **Nydia Morales-Soto**[b,c], **Sage J.B. Dunham**[d], **Jonathan V. Sweedler**[d], **Joshua D. Shrout**[b,c], and **Paul W. Bohn**[a]

[a]Department of Chemistry & Biochemistry and Department of Chemical and Biomolecular Engineering, University of Notre Dame, Notre Dame, IN 46556, USA

[b]Department of Civil and Environmental Engineering and Earth Sciences and Department of Biological Sciences, University of Notre Dame, Notre Dame, IN 46556, USA

[c]Eck Institute for Global Health, University of Notre Dame, USA

[d]Department of Chemistry and Beckman Institute for Advanced Science and Technology, University of Illinois at Urbana-Champaign, Urbana, IL 61801, USA

Abstract

Biofilms, such as those formed by the opportunistic human pathogen *Pseudomonas aeruginosa* are complex, matrix enclosed, and surface-associated communities of cells. Bacteria that are part of a biofilm community are much more resistant to antibiotics and the host immune response than their free-floating counterparts. *P. aeruginosa* biofilms are associated with persistent and chronic infections in diseases such as cystic fibrosis and HIV-AIDS. P. aeruginosa synthesizes and secretes signaling molecules such as the Pseudomonas quinolone signal (PQS) which are implicated in quorum sensing (QS), where bacteria regulate gene expression based on population density. Processes such as biofilms formation and virulence are regulated by QS. This manuscript describes the powerful molecular imaging capabilities of confocal Raman microscopy (CRM) and surface enhanced Raman spectroscopy (SERS) in conjunction with multivariate statistical tools such as principal component analysis (PCA) for studying the spatiotemporal distribution of signaling molecules, secondary metabolites and virulence factors in biofilm communities of *P. aeruginosa*. Our observations reveal that the laboratory strain PAO1C synthesizes and secretes 2-alkyl-4-hydroxyquinoline N-oxides and 2-alkyl-4-hydroxyquinolones in high abundance, while the isogenic acyl homoserine lactone QS-deficient mutant (*ΔlasIΔrhlI*) strain produces predominantly 2-alkyl-quinolones during biofilm formation. This study underscores the use of CRM, along with traditional biological tools such as genetics, for studying the behavior of microbial communities at the molecular level.

Keywords

Raman spectroscopy; *Pseudomonas aeruginosa*; biofilms; quinolones; phenazines

1. INTRODUCTION

Biofilms of the pathogenic bacterium *Pseudomonas aeruginosa* are associated with severe and persistent infections in patients afflicted with diseases such as cystic fibrosis (CF) and HIV-AIDS, leading to a high rate of mortality and morbidity among such patients[1]. The formation of biofilms of *P. aeruginosa* proceeds via a complex series of mechanisms. One such mechanism implicated in biofilm formation in *P. aeruginosa* is quorum sensing (QS). QS involves regulation of gene expression in response to the accumulation of cell-cell signaling molecules secreted by a certain "quorum" or population of bacteria.[2–3] In *P. aeruginosa*, biofilm formation, the synthesis of virulence factors and secondary metabolites is regulated via a system of interconnected QS systems namely, *rhl*, *las* and *pqs*. The *las* and *rhl* QS systems are activated by N-acyl homoserine lactones while the *pqs* system is operated by a distinct class of aromatic signaling molecules called quinolones.[4] *P. aeruginosa* synthesizes and secretes over 50 different types of quinolones, the most noteworthy of which are 2-heptyl-3-hydroxy-4-quinolone, also referred to as the Pseudomonas quinolone signal (PQS), and its immediate precursor 2-heptyl-4-(1H)-quinolone (HHQ).[5–6] In addition to the development of biofilms, surface motility and membrane vesicle formation, PQS has been implicated in the production of the blue, heterocyclic nitrogen containing virulence factor pyocyanin.[7–8] Pyocyanin is present in high abundance (upto 100μM) in the sputum of CF patients and is often linked to progressive lung damage in CF patients suffering from *P. aeruginosa* infections.[9–10]

The vast impact of *P. aeruginosa* on human health coupled with the inherent structural and molecular complexity of its biofilm communities, necessitates the development of analytical tools for characterizing the spatial and temporal distribution of signaling molecules, metabolites and virulence factors secreted by the bacteria, at the molecular level. Confocal Raman microscopy (CRM) is one such powerful analytical tool that can be applied to probe the chemical dynamics of heterogeneous biological systems.[11–12] The use of CRM provides sub-micron (diffraction limited) spatial resolution for constructing 3D chemical maps of the biological sample under study.[13–14] For example, CRM imaging has been employed extensively in the biomedical sciences for studying the distribution of biomolecules within living cells, the diagnosis of cancer *in vivo* and identification of cancer biomarkers.[15–18] Furthermore, compared to normal Raman spectroscopy, surface enhanced Raman spectroscopy (SERS) provides higher sensitivity along with the ability to probe biological samples exhibiting high auto-fluorescence.

The current work highlights the label-free imaging capability of CRM and SERS in conjunction with principal component analysis (PCA) for analyzing the distribution of quinolone signaling molecules and secondary metabolites in biofilms of *P. aeruginosa* wild-type, QS-deficient mutant and CF isolate strains. In addition, this study also underscores the advantages of using molecular imaging methods along with traditional microbiological tools for studying biochemical phenomena.

2. METHODS

2.1 Materials

Silicon substrates were purchased from WRS Materials (San Jose, CA) as 3-in-diameter wafer of Si (100), then scored and broken into 2×2 cm^2 tiles before use. Pyocyanin and quinolone standards: 2-heptyl-3-hydroxy-4(1H)-quinolone (Pseudomonas quinolone signal, PQS) and 2-heptyl-4-quinolone (HHQ), were purchased from SigmaAldrich (St Louis, MO) while 4-hydroxy-2-heptylquinoline-*N*-oxide (HQNO) was purchased from Enzo Life Sciences (Farmingdale, NY). The standards were dissolved in HPLC-grade ethanol (Sigma-Aldrich), then deposited and air-dried on clean Si wafers for the Raman measurements. Sodium borohydride ($NaBH_4$) and silver nitrate ($AgNO_3$) were also purchased from Sigma Aldrich and used without further purification.

2.3 Colloid Synthesis

Colloidal silver solutions were prepared according to the standard protocol established by Lee and Miesel which resulted in 12–14nm nanoparticles.[19]

2.2 Biofilm Culture Methods

P. aeruginosa strains PAO1C, isogenic QS mutant deficient for AHL production and for rhamnolipid secretion (Δ*lasI*Δ*rhlI*)[2], and FRD1 (CF lung isolate)[20] were used in this study. Cell cultures were grown overnight at 37°C with shaking at 240 rpm in modified Fastidious Anaerobe Broth (FAB) culture medium supplemented with 30 mM filter sterilized glucose as the source of carbon.

To grow static biofilms, 200 μL of overnight broth culture (OD = 1 at 600 nm) was pipetted onto either a 2 cm × 2 cm sterilized Si tile or gold coated Si tile placed in a Petri dish (each Petri dish holding three tiles). After allowing 10–15 min for bacterial attachment, the inoculated Si tiles were immersed in 18 mL of fresh FAB medium containing 450 μL of 1.2 M glucose and incubated at 37 °C until the desired growth time had elapsed. The tiles containing bacterial growth were carefully removed from the petri dish with sterile tweezers and allowed to dry for ~1 h in a hood.

Pellicle biofilms (biofilms that form at the air-liquid interface) were grown in a test tube by inoculating 6 mL of fresh FAB medium containing 150 μL of 1.2 M glucose, with 200 μL of the overnight cell culture (OD=1 at 600nm) followed by incubation (without shaking) at 37°C until the desired time of growth had elapsed. For SERS analysis 50 μL of the growth at the air-liquid interface was transferred to a sterile silicon tile, and 100 μL of silver colloid was added to the sample and allowed to dry in the dark.[21–22]

2.4 Raman measurements and Data Analysis

Raman analysis was performed using a laser scanning confocal Raman microscope (Alpha 300R, WITec, GMBH, Germany), equipped with 532 and 785 nm focused lasers. The laser radiation was delivered to the microscope using a polarization preserving single mode optical fiber, deflected through a dichroic beam-splitter and focused onto the sample through the microscope objectives. Raman images from biofilms were acquired using either a

coverslip corrected Nikon water immersion 60× objective (NA = 1) or a 40× air objective (NA = 0.6). Images were obtained by acquiring a full Raman spectrum from each image pixel (150 × 150, 100×100 or 80×80 pixels) over a desired region on the sample with an integration time of 100 ms per spectrum. Data processing software WITec Project 2.10 was used to remove cosmic ray spikes from Raman images. Principal component analysis was performed on the Raman images in MATLAB using previously established procedures.[23]

3. RESULTS AND DISCUSSION

3.1 Characterization of quinolones/quinolines in static biofilms of *P. aeruginosa* wild-type, QS-mutant and cystic fibrosis isolate strains

The distributions of quinolone signaling molecules and quinoline secondary metabolites were mapped in 2-day static biofilms of *P. aeruginosa* wild-type and QS-deficient mutant with Raman microspectroscopy. Raman spectra generated from regions of high quinolone/quinolone abundance from biofilms of both strains exhibited a very strong band between 1338–1376 cm^{-1}, which is attributed to the quinolone ring stretch vibration. In addition to the quinolone ring stretch, other vibrations associated with the quinolone ring were also observed in the Raman spectra, for example, −CH bending/twisting and C–O stretching centered at ~1205 cm^{-1} pyridine ring stretch vibrations in the 1550–1600 cm^{-1} region, and symmetric ring breathing vibrations of the aromatic ring at ~715 cm^{-1}.[24–26]

Raman images, integrated over the 1338–1376 cm^{-1} filter, representative of the quinolone ring stretch vibration, were acquired from regions of high quinolone/quinoline abundance within the biofilm matrix. Subsequent principal component (PC) analysis of the Raman images generated PC loading plots that resemble spectra of quinolone/quinoline standards. PC loading plots generated from Raman images obtained from wild-type *P. aeruginosa* biofilms revealed the presence of two chemically distinct yet co-localized analytes within the biofilm matrix. PC1 (Figure 2B) exhibits a set of features with peaks at ~1372, 1461, 1556, and 1591 cm^{-1}, that resemble the spectrum of PQS standard (Figure 1) while PC2 (Figure 2D) exhibits features with peaks at 1357, 679, 715, 1205, 1435 and 1511 cm^{-1}, that bear a striking resemblance to the spectrum of HQNO standard (Figure 1). Other analytes, if present within the imaged regions, were below the limit of detection of CRM.[27]

On the other hand, PC2 loading plot (Figure 3B) generated from similar analysis of Raman images collected from 2-day biofilms of QS-deficient mutant strain (Figure 3A) reveals features with distinct peaks at ~1354, 1503, and 1171 cm^{-1}. This particular set of features is consistent with the presence of the HHQ family of quinolones, as evidenced by the congruence between the features in the PC1 loading plot and the spectrum of HHQ standard (Figure 1). The observation that HHQ family of quinolones dominates the QS mutant biofilms versus the wild-type biofilm is consistent with the fact that HHQ is a precursor to PQS and the conversion of HHQ to PQS is regulated by the *las* QS system. Therefore, in the Δ*lasI*Δ*rhlI* mutant strain the HHQ family rather than the PQS family of quinolones is secreted in high abundance.[28]

FRD1 biofilms exhibit significant auto-fluorescence, more so than PAO1C biofilms, presumably due to a greater abundance of fluorescent pigments secreted by the bacteria,

such as the siderophore pyoverdin, which absorb light in the visible region of the electromagnetic spectrum.[29–30] Contribution from fluorescence background can completely obstruct Raman signals, especially when Raman measurements are performed with a visible 532 nm laser[31] (Figure 4). Therefore, in order to circumvent interference from auto-fluorescence in FRD1 biofilms, Raman measurements were performed using a 785 nm near infra-red laser.

Raman images collected from quinolone "pools" in FRD1 static biofilms were integrated over 1359–1393 cm^{-1} filter to construct false colored images, one such image being shown in Figure 5(A). Subsequent PC analysis of the Raman image generated a PC2 loading plot (Figure 5(B)) that bears features with peaks at ~1370, 1155 and 1597 cm^{-1}, reminiscent of the vibrational bands from the Raman spectrum of PQS standard (Figure 1).

Furthermore, PQS and HHQ spectral signatures generated from the biofilm matrix exhibit a strong band between 1638–1676 cm^{-1}, which is assigned to a combined amide I stretch indicative of proteins and C=C stretch from unsaturated lipids.[15] The presence of the strong 1638–1676 cm^{-1} band in PQS and HHQ biofilm associated spectral signatures could be attributed to the fact that PQS and HHQ family of quinolones are packaged and transported in outer membrane vesicles, which are lipopolysaccharide structures derived from the bacterial cell membrane that deliver small molecule metabolites, proteins and DNA to bacterial cells.[32]

3.2 SERS Characterization of pyocyanin in pellicle biofilms of CF isolate strain FRD1

SERS imaging was employed for the *in situ* characterization of pyocyanin, which is an important virulence factor and biomarker for *P. aeruginosa* infection, in pellicle biofilms of FRD1. PC1 loading plot (Figure 6A) generated from the analysis of the SERS image from a 2-day FRD1 pellicle biofilm (Figure 6B) reveals features at ~1352, 1511, 1572 and 1600 cm^{-1}.[22] These high z-score features resemble SERS bands representing a combined C-C/C-N stretch and C-H bend at 1352 cm^{-1}, C-C stretch, CH_3 wag and C-H in-plane bend at 1511 cm^{-1} present in the SERS spectrum of pyocyanin standard[33] (Figure 6A inset).

4. CONCLUSION

In this paper we describe the application of CRM and SERS for the *in situ* characterization of quinolone/quinoline signaling molecules and phenazine secondary metabolites synthesized and secreted by *P. aeruginosa* in biofilm communities. Furthermore, we show that challenges associated with Raman analysis of biological samples namely, sample auto-fluorescence and low sensitivity of Raman scattering may be circumvented by conducting Raman measurements in the near infra-red with a 785nm laser or employing SERS using silver nanoparticles. Finally, we also demonstrate the efficacy of CRM analysis in conjunction with PCA for non-invasively characterizing the products of genetic alteration in the *P. aeruginosa* QS-deficient mutant strain, which secretes mainly HHQ family of quinolones, since it lacks the genes involved in the production of the enzyme implicated in the conversion of HHQ to PQS. The outcome of this study underscores the usefulness of CRM for studying biochemical processes involved in the formation and growth of biofilms of *P. aeruginosa* at the molecular level.

Acknowledgments

This work was supported by the National Institute of Health grant 1R01AI113219-01 and by the Department of Energy through a subcontract from Oak Ridge National Laboratory (PTX-UT-Battelle), grant ORNL-4000132808 (SP). The authors would also like to thank the Advanced Diagnostics & Therapeutics initiative at the University of Notre Dame for partial support.

References

1. Costerton JW, Stewart PS, Greenberg EP. Bacterial biofilms: a common cause of persistent infections. Science. 1999; 284(5418):1318–1322. [PubMed: 10334980]
2. Shrout JD, Chopp DL, Just CL, Hentzer M, Givskov M, Parsek MR. The impact of quorum sensing and swarming motility on Pseudomonas aeruginosa biofilm formation is nutritionally conditional. Mol Microbiol. 2006; 62(5):1264–1277. [PubMed: 17059568]
3. Miller MB, Bassler BL. Quorum sensing in bacteria. Annu Rev Microbiol. 2001; 55(165–199)
4. McGrath S, Wade DS, Pesci EC. Dueling quorum sensing systems in Pseudomonas aeruginosa control the production of the Pseudomonas quinolone signal (PQS). FEMS Microbiol Lett. 2004; 230(1):27–34. [PubMed: 14734162]
5. Reen FJ, Mooij MJ, Holcombe LJ, McSweeney CM, McGlacken GP, Morrissey JP, O'Gara F. The Pseudomonas quinolone signal (PQS), and its precursor HHQ, modulate interspecies and interkingdom behaviour. FEMS Microbiol Ecol. 2011; 77(2):413–428. [PubMed: 21539583]
6. Heeb S, Fletcher MP, Chhabra SR, Diggle SP, Williams P, Camara M. Quinolones: from antibiotics to autoinducers. FEMS Microbiol Rev. 2011; 35(2):247–274. [PubMed: 20738404]
7. Dietrich LE, Petersen APrice-Whelan, A, Whiteley M, Newman DK. The phenazine pyocyanin is a terminal signalling factor in the quorum sensing network of Pseudomonas aeruginosa. Mol Microbiol. 2006; 61(5):1308–1321. [PubMed: 16879411]
8. Diggle SP, Cornelis P, Williams P, Camara M. 4-quinolone signalling in Pseudomonas aeruginosa: old molecules, new perspectives. Int J Med Microbiol. 2006; 296(2–3):83–91. [PubMed: 16483840]
9. Caldwell CC, Chen Y, Goetzmann HS, Hao Y, Borchers MT, Hassett DJ, Young LR, Mavrodi D, Thomashow L, Lau GW. Pseudomonas aeruginosa exotoxin pyocyanin causes cystic fibrosis airway pathogenesis. Am J Pathol. 2009; 175(6):2473–2488. [PubMed: 19893030]
10. Rada B, Leto TL. Pyocyanin effects on respiratory epithelium: relevance in Pseudomonas aeruginosa airway infections. Trends Microbiol. 2013; 21(2):73–81. [PubMed: 23140890]
11. Petry R, Schmitt M, Popp J. Raman spectroscopy–a prospective tool in the life sciences. Chemphyschem. 2003; 4(1):14–30. [PubMed: 12596463]
12. Sandt C, Smith-Palmer T, Pink J, Brennan L, Pink D. Confocal Raman microspectroscopy as a tool for studying the chemical heterogeneities of biofilms in situ. J Appl Microbiol. 2007; 103(5): 1808–1820. [PubMed: 17953591]
13. Masyuko R, Lanni EJ, Sweedler JV, Bohn PW. Correlated imaging–a grand challenge in chemical analysis. Analyst. 2013; 138(7):1924–1939. [PubMed: 23431559]
14. Ellis DI, Cowcher DP, Ashton L, O'Hagan S, Goodacre R. Illuminating disease and enlightening biomedicine: Raman spectroscopy as a diagnostic tool. Analyst. 2013; 138(14):3871–3884. [PubMed: 23722248]
15. Notingher I, Verrier S, Haque S, Polak JM, Hench LL. Spectroscopic study of human lung epithelial cells (A549) in culture: living cells versus dead cells. Biopolymers. 2003; 72(4):230–240. [PubMed: 12833477]
16. Hamada K, Fujita K, Smith NI, Kobayashi M, Inouye Y, Kawata S. Raman microscopy for dynamic molecular imaging of living cells. J Biomed Opt. 2008; 13(4):044027. [PubMed: 19021354]
17. Stone N, Kendall C, Smith J, Crow P, Barr H. Raman spectroscopy for identification of epithelial cancers. Faraday Discuss. 2004; 126:141–157. discussion 169–183. [PubMed: 14992404]
18. Li M, Cushing SK, Zhang J, Suri S, Evans R, Petros WP, Gibson LF, Ma D, Liu Y, Wu N. Three-dimensional hierarchical plasmonic nano-architecture enhanced surface-enhanced Raman

scattering immunosensor for cancer biomarker detection in blood plasma. ACS Nano. 2013; 7(6): 4967–4976. [PubMed: 23659430]

19. Lee PC, Meisel D. Adsorption and surface-enhanced Raman of dyes on silver and gold sols. The Journal of Physical Chemistry. 1982; 86(17):3391–3395.
20. Ohman DE, Chakrabarty AM. Genetic mapping of chromosomal determinants for the production of the exopolysaccharide alginate in a Pseudomonas aeruginosa cystic fibrosis isolate. Infect Immun. 1981; 33(1):142–148. [PubMed: 6790439]
21. Spiers AJ, Bohannon J, Gehrig SM, Rainey PB. Biofilm formation at the air-liquid interface by the Pseudomonas fluorescens SBW25 wrinkly spreader requires an acetylated form of cellulose. Mol Microbiol. 2003; 50(1):15–27. [PubMed: 14507360]
22. Polisetti S, Baig NF, Morales-Soto N, Shrout JD, Bohn PW. Spatial Mapping of Pyocyanin in Pseudomonas Aeruginosa Bacterial Communities Using Surface Enhanced Raman Scattering. Appl Spectrosc. 2016
23. Ahlf DR, Masyuko RN, Hummon AB, Bohn PW. Correlated mass spectrometry imaging and confocal Raman microscopy for studies of three-dimensional cell culture sections. Analyst. 2014; 139(18):4578–4585. [PubMed: 25030970]
24. Neugebauer U, Szeghalmi A, Schmitt M, Kiefer W, Popp J, Holzgrabe U. Vibrational spectroscopic characterization of fluoroquinolones. Spectrochim Acta A Mol Biomol Spectrosc. 2005; 61(7):1505–1517. [PubMed: 15820884]
25. Wang Y, Yu K, Wang S. Vibrational spectra study on quinolones antibiotics. Spectrochim Acta A Mol Biomol Spectrosc. 2006; 65(1):159–163. [PubMed: 16504572]
26. Frosch T, Popp J. Relationship between molecular structure and Raman spectra of quinolines. Journal of Molecular Structure. 2009; 924–926:301–308.
27. Baig NF, Dunham SJ, Morales-Soto N, Shrout JD, Sweedler JV, Bohn PW. Multimodal chemical imaging of molecular messengers in emerging Pseudomonas aeruginosa bacterial communities. Analyst. 2015; 140(19):6544–6552. [PubMed: 26331158]
28. Lanni EJ, Masyuko RN, Driscoll CM, Aerts JT, Shrout JD, Bohn PW, Sweedler JV. MALDI-guided SIMS: multiscale imaging of metabolites in bacterial biofilms. Anal Chem. 2014; 86(18): 9139–9145. [PubMed: 25133532]
29. Moon CD, Zhang XX, Matthijs S, Schafer M, Budzikiewicz H, Rainey PB. Genomic, genetic and structural analysis of pyoverdine-mediated iron acquisition in the plant growth-promoting bacterium Pseudomonas fluorescens SBW25. BMC Microbiol. 2008; 8(7)
30. Haas B, Kraut J, Marks J, Zanker SC, Castignetti D. Siderophore presence in sputa of cystic fibrosis patients. Infect Immun. 1991; 59(11):3997–4000. [PubMed: 1834571]
31. Ivleva NP, Wagner M, Szkola A, Horn H, Niessner R, Haisch C. Label-free in situ SERS imaging of biofilms. J Phys Chem B. 2010; 114(31):10184–10194. [PubMed: 20684642]
32. Wessel AK, Liew J, Kwon T, Marcotte EM, Whiteley M. Role of Pseudomonas aeruginosa Peptidoglycan-Associated Outer Membrane Proteins in Vesicle Formation. Journal of Bacteriology. 2013; 195(2):213–219. [PubMed: 23123904]
33. Wu X, Chen J, Li X, Zhao Y, Zughaier SM. Culture-free diagnostics of Pseudomonas aeruginosa infection by silver nanorod array based SERS from clinical sputum samples. Nanomedicine. 2014; 10(8):1863–1870. [PubMed: 24832961]

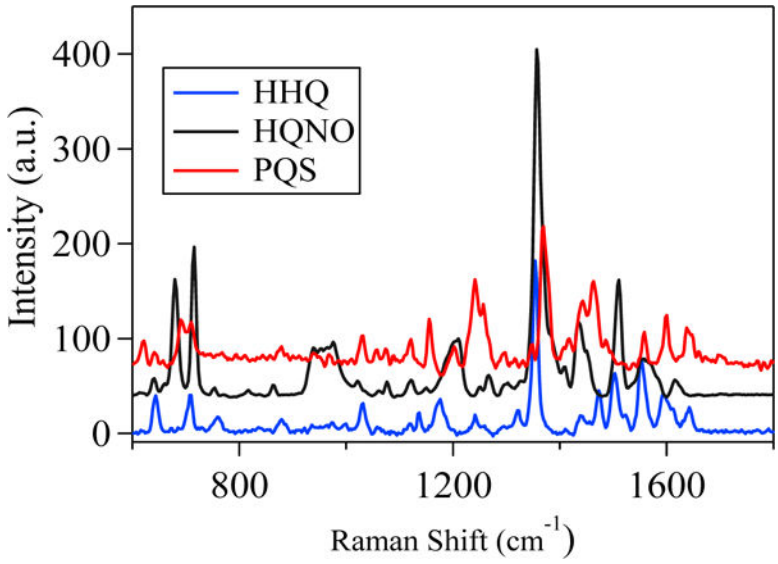

Figure 1.
Raman spectra of quinolone standards: HHQ, HQNO and PQS.

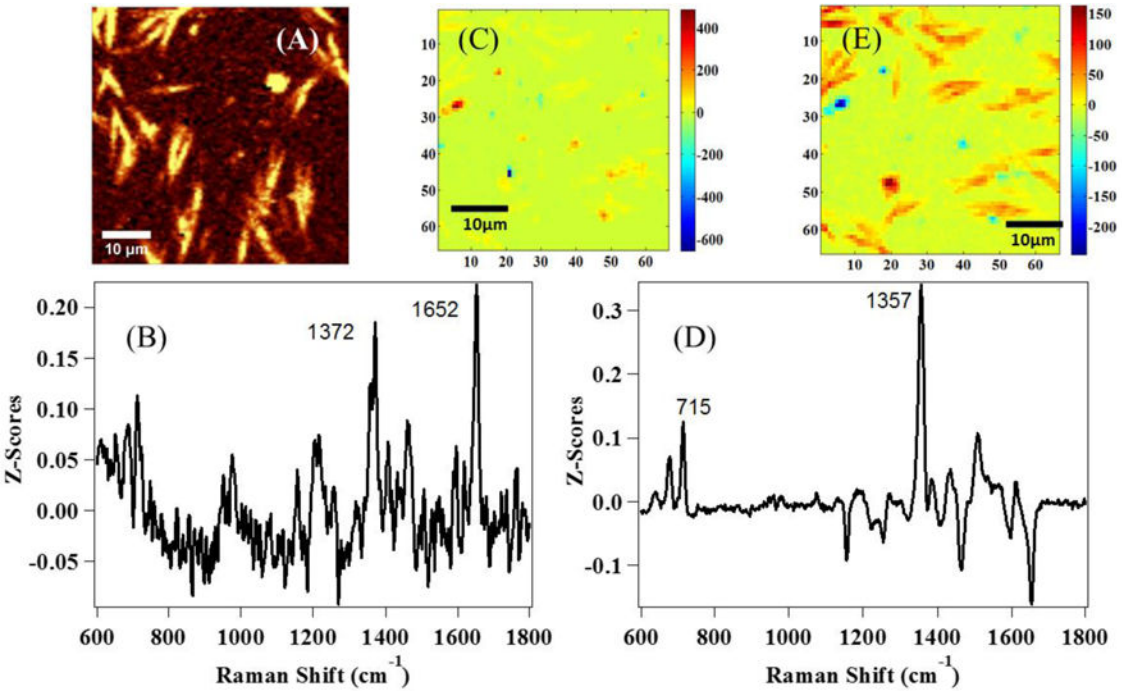

Figure 2.

(A) Raman image acquired from a 2-day PAO1C biofilm constructed from a 1338–1376 cm $^{-1}$ filter; (B) PC1 and (D) PC2 loading plots generated from PC analysis of Raman image in (A); (C) and (E) heat maps showing the distribution of PC1 and PC2, respectively.

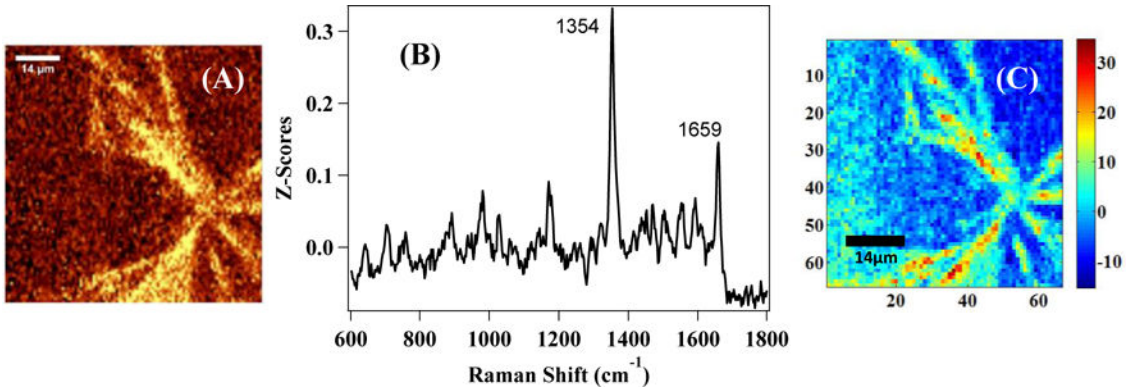

Figure 3.

(A) Raman image acquired from a 2-day QS-deficient mutant biofilm constructed from a 1338–1376 cm^{-1} filter; (B) PC1 loading plot generated from PC analysis of Raman image in (A); (C) heat map showing the distribution of PC1.

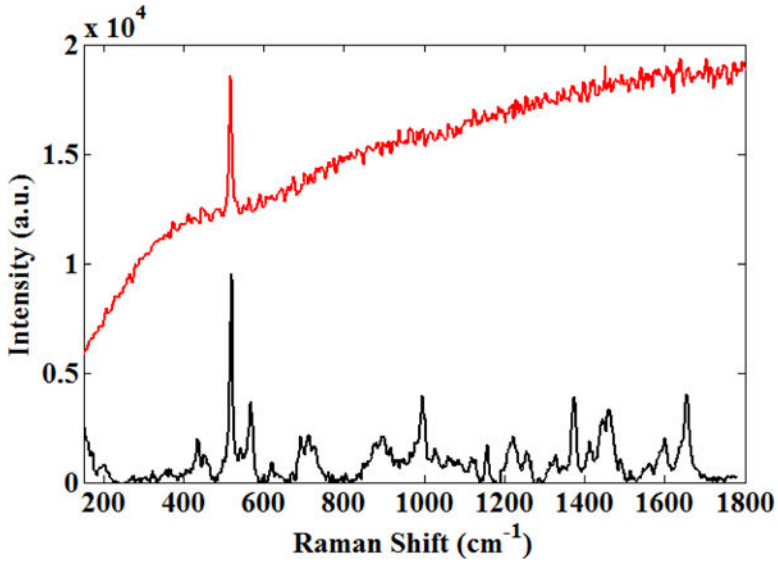

Figure 4.

Comparison of representative spectra generated from FRD1 static biofilms. The spectra in red was collected using 532nm laser while the spectra in black was collected with a 785nm laser.

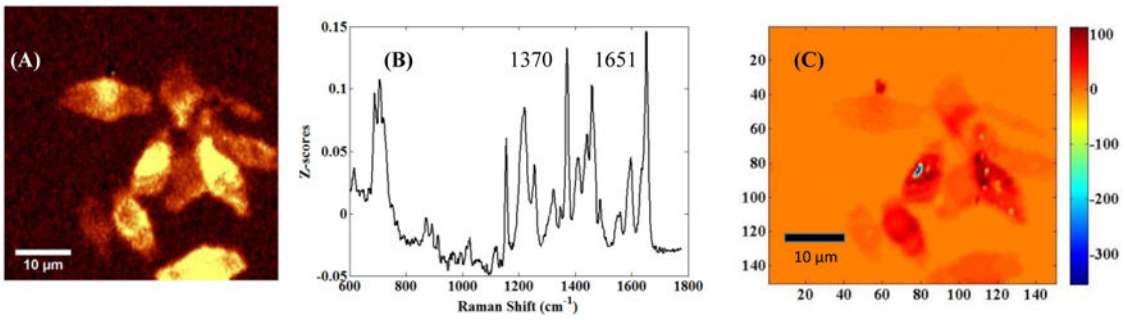

Figure 5.

(A) Raman image acquired from a 2-day FRD1 static biofilm constructed from a 1359–1393 cm^{-1} filter; (B) PC1 loading plot generated from PC analysis of Raman image in (A); (C) heat map showing the distribution of PC1.

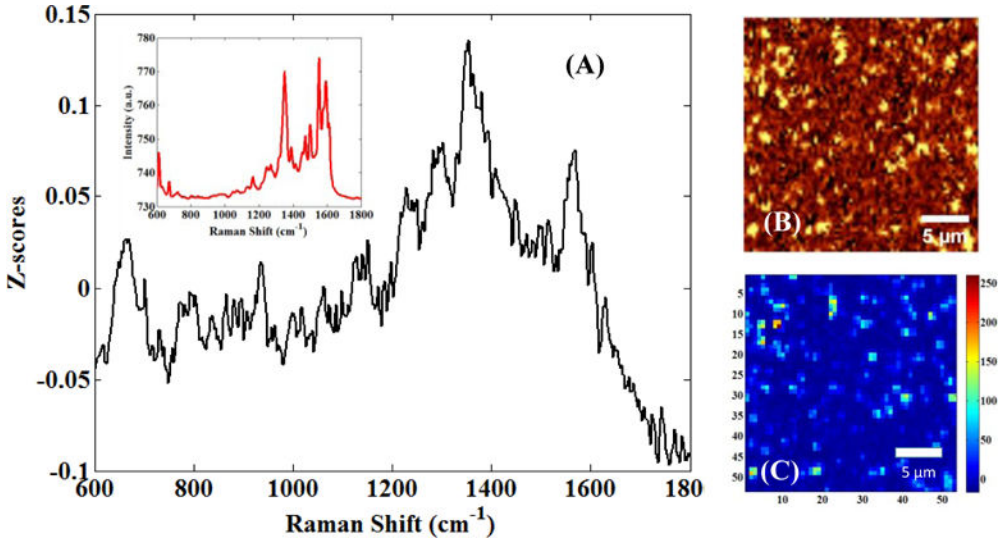

Figure 6.

(A) PC1 loading plot generated from PC analysis of Raman image (B) obtained from a 2-day pellicle biofilm of FRD1 and integrated over 1320–1400 cm^{-1} to include the strong marker band for pyocyanin at ~1354 cm^{-1}; (C) heat map showing the distribution of PC1. The SERS spectrum of pyocyanin standard is shown in (A) inset.